

# FT-ICR mass spectrometry: Superconducting magnet, external ion source, ion–molecule reactions, and ion–ion traps

Karl Peter Wanczek<sup>1</sup> | Basem Kanawati<sup>2</sup>

<sup>1</sup>Institute of Physical and Inorganic Chemistry, University of Bremen, FB 2, Bremen, Germany

<sup>2</sup>Research Unit Analytical BioGeoChemistry, Helmholtz Zentrum München, Neuherberg, Germany

## Correspondence

Basem Kanawati, Research Unit Analytical BioGeoChemistry, Helmholtz Zentrum München, Ingolstaedter Landstrasse 1, Neuherberg D-85764, Germany.

Email: [basem.kanawati@helmholtz-muenchen.de](mailto:basem.kanawati@helmholtz-muenchen.de)

This paper is dedicated to Alan Marshall in recognition of his contributions to the field of ICR mass spectrometry.

## Abstract

The world of Fourier-transform ion cyclotron resonance (FT-ICR) mass spectrometry has witnessed, especially in the last 30 years significant advances in many fields of science, such as electronics, magnets, new ICR cell designs, developed ICR event sequences, modern external ionization sources, and linear ion beam guides, as well as modern vacuum technology. In this review, a brief account is given focusing especially on the studies performed in Wanczek's group and ICR research laboratory at the University of Bremen. An FT-ICR mass spectrometer has been developed with a high magnetic field superconducting magnet, operating at 4.7 T. At this magnetic field, a trapping time of 13.5 h was obtained with 30% efficiency. For the tetrachloromethane molecular ion,  $m/z$  166, a mass-resolving power  $m/\Delta m = 1.5 \times 10^6$  was measured at a pressure of  $2 \times 10^{-8}$  Torr. The transition from magnet sweep to frequency sweep and the application of Fourier-transform has greatly enhanced the ICR technology. External ion sources were invented and differential pumping schemes were developed for enabling ultrahigh vacuum condition for ICR detection, while guiding ions at relatively higher pressures, during their flight to the ICR cell. With the external ion source, a time-of-flight ICR tandem instrument is built. A method to measure the ion flight time and to trap the ions in the ICR cell is described. Many ICR cell characteristics such as  $z$ -axis ion ejection and coupling of radial and axial ion motions in a superposed homogeneous magnetic and inhomogeneous trapping electric field were extensively studied. Gas-phase ion–molecule reactions of several reactive inorganic compounds with a focus on phosphorous and sulfur as well as silicon chemistry were also studied in great detail. The gas-phase ion chemistry of several trifluoromethyl-reagents such as trifluoromethyltrimethylsilane and tris(trifluoromethyl)phosphine were also investigated in ICR. Dual polarities multisegmented ICR cells were invented and deeply characterized. Sophisticated ICR pulse event programs were developed to enable long-range ion–ion interactions between simultaneously trapped positive and negative ions.

## KEYWORDS

axial motion, dual polarities cell, external ion source, ICR, ion–ion interaction, ion–molecule, radial motion, superconducting magnet, time of flight

## 1 | INTRODUCTION

Ion motion under the influence of magnetic and electric fields was the subject of many reviews in the past (Hendrickson & Emmett, 1999; Marshall et al., 1998; Marshall & Chen, 2015; Nikolaev et al., 2016; Nolting et al., 2019). Ion detection principles in ICR were thoroughly reviewed and many experimental configurations were discussed (Marshall & Hendrickson, 2002). Therefore, only a brief description of the ICR technique will be made here. Ions can be trapped in an ICR cell by the application of superposed magnetic and electric fields. A pure magnetic field can only confine ions in the radial plane ( $XY$ ), which is perpendicular to the magnetic field lines ( $Z$ ). With the absence of an electric field, produced generally by applying an electric voltage on both trapping electrodes of the ICR cell, ions can axially drift in both  $Z$ -directions along the magnetic field lines and can subsequently migrate out of the cell. Thus, an axial component of the electric field is important to ensure the three-dimensional (3D) confinement of ions inside the cell. However, applying a trapping electric field alters the pure cyclotron frequency (which originated from the pure magnetic field in an absence of any imposed electric field). The resulting “modified” cyclotron frequency due to the existence of the trapping electric field is defined as “reduced” cyclotron frequency. In the past, ion detection was focused on measuring the single reduced cyclotron frequency. However, Nikolaev et al. (1985) succeeded to register a Soviet Union's patent in 1985, where multi-electrode detection schemes could be invented at that time to detect the double and the triple of the reduced cyclotron frequencies of the trapped ions inside ICR cells.

After that, a trend toward utilization of the double-reduced cyclotron frequency has emerged. Doubling the detected cyclotron frequency has definitely a key advantage of increasing the mass-resolving power in the generated mass spectra. In a dipolar detection mode, two time-domain transients are produced from the pair of detection electrodes, located perpendicular to the magnetic field lines. Schweikhard et al. (1989) invented new detection schemes by taking the sum of these two time-domain transients, instead of their difference, performed a Fourier-transform on it, and could obtain a signal representing the double value of the reduced cyclotron frequency  $\omega_+$  of  $N_2^+$  ions trapped in a Penning trap. They showed that this is valid only when the cyclotron radius

is greater than the magnetron radius of the trapped ions. The signal decreases in intensity when the magnetron radius becomes bigger than the cyclotron radius. With larger magnetron radii of the trapped ions, it is possible to obtain both  $\omega_+ - \omega_-$  as well as  $\omega_+ + \omega_-$ . The latter term represents the pure “unperturbed” cyclotron frequency  $\omega_c$ , which is obtained in the absence of any trapping electric field and it is of particular importance for accurate mass measurement studies. One year later, Schweikhard et al. (1990) could extend this detection scheme to enable quadrupolar detection in Fourier-transform ion cyclotron resonance mass spectrometry (FT-ICR-MS) by utilizing two detection pairs of opposite electrodes and taking the difference of their summed transients. With this approach, very high signal intensities of trapped and excited argon ions could be obtained at the unperturbed pure cyclotron frequency  $\omega_c = \omega_+ + \omega_-$ , which is experimentally validated to be indeed independent on the trapping electric voltages.

Marshall and Hendrickson (2008) wrote an extensive review about high-resolution mass spectrometers, emphasizing the capabilities of these instruments based on the  $m/z$  ratio of the trapped ions in a wide mass range from small metabolites to intact proteins. Forcisi et al. (2013) reviewed the key role of LC coupling to high-resolution mass analyzers for metabolic research. Hartmann et al. (1980) performed an intensive quantum mechanical study for characterizing the Coriolis coupling of the ion cyclotron motion to ion internal degrees of freedom. Mass calibration for accurate mass measurements and digital signal processing were also reviewed in detail (Kanawati et al., 2019; Zhang et al., 2005). Wanczek and colleagues covered in many reviews and book chapters the physics of ions inside superposed magnetic and electric fields (Hartmann et al., 1973, 1983; Hartmann & Wanczek, 1978, 1982; Lee et al., 1980; Wanczek, 1982, 1989) and showed many applications to this technique in the field of gas-phase ion chemistry. In this review, specific developments topics concerning ICR-MS will be discussed in detail, shedding the light on the key outcomes of such developments and their contribution to enhance the ICR technology.

Besides ion detection in ICR, ion trajectory stability is required for both pre-excitation as well as after radial ion excitation prior to signal detection. There were some challenges in the past to increase ion trapping efficiency before radial ion excitation and also to reduce the radial electric

field applied on ions after their radial excitation prior to detection. For these reasons, it was important for Wanczek's group to develop sophisticated ICR cell experiments with a 4.7-T superconducting magnet in the 80s as will be described in some detail in the next section. Before 1985, almost all ionization processes were done inside the low-pressure region of the ICR cell, by the use of rhenium high current filament and electric voltage accelerator to let electrons impact the neutrals inside the ICR cell with 70eV kinetic energy, in what is defined as electron impact (EI) ionization. However, the heated filament caused the base pressure inside the ICR cell region to increase due to degassing effects, which affected the mass resolution of detected ions. A sudden burst in that filament can even break the ultrahigh vacuum (UHV) in the FT-ICR-MS vacuum chamber. Moreover, it was important to allow for externally generated ions to overcome the magnetic fringing fields and enter the ICR cell from outside because this allows for other ionization sources to be integrated with the FT-ICR-MS technique. Even electron-impact based external ionization sources are favored over internal EI filament source inside the ICR cell due to enhanced vacuum in the ICR cell region when an external EI source is integrated.

Along with the developments of the linear ion path for integration of an external ion source in Wanczek's group, ion flight time dependency on the  $m/z$  ratio of linearly moving ions from the external ion source to the ICR cell was discerned. This fact was utilized at that time to limit the  $m/z$  range of ions that can further move to the ICR cell, which lead to increased dynamic range and also enhanced the mass-resolving power of detected signals due to reduction of the space-charge effect of trapped ions inside the ICR cell.

Gas-phase ion-molecule reactions investigations were also one of the main interests of Wanczek's group in the 80s and 90s of the previous century. New reaction product ions were investigated and reaction rate constants were determined by ICR, thanks to its capability to run in double-resonance ion excitation mode. For the sake of ion-molecule reactions to be studied accurately, ion loss due to any physical mean inside the ICR cell should be excluded. It was, therefore, a main goal for Wanczek's group to study the mechanisms of axial ion ejection during radial ion excitation and also to investigate coupling mechanisms of radial and axial motions of trapped ions inside ICR cells.

The last research interest in Wanczek's group was the development of multi-section elongated open cylindrical ICR cells with exact and different trapping electrode diameters, to study double-well electric potential configurations for simultaneous trapping and detection of positive and negative ions. A further goal was also the investigation of long-range ion-ion interactions between positive and negative ions, simultaneously trapped in neighboring ion

stability regions of the multi-section ICR cell. Although no electron transfer ion-ion reaction was observed in those cells, a deep analysis of the factors, which present a barrier against an electron transfer to be observed was done. Details about all these interesting ICR investigations will be given in the next few sections of this review.

## 2 | SUPERCONDUCTING MAGNET FOR FT-ICR-MS

ICR-MS is well known to provide the highest mass-resolving power when compared to any other mass analyzer. This is due to the very long ion flight path, which can be achieved by cyclotron motion. However, the mass resolution in ICR is linearly proportional to the magnetic field strength. Thus, a need for high magnetic fields is always necessary to obtain high frequency and thus mass resolution, as they increase proportionally with the magnetic field strength. High magnetic fields can also allow for better ion detection sensitivity and lead to the expanded mass range, due to enabling an increased upper mass limit, as the upper mass limit increases proportionally to the square of the magnetic field induction  $B$ . It is well-known that ions inside ICR can be excited to higher kinetic energies with increasing magnetic field  $B$ . Given the same cyclotron radius, the translational kinetic energy of trapped ions inside ICR is proportional to the square of the magnetic field induction  $B$ . Moreover, confined ions inside ICR have lower thermal cyclotron radii, when  $B$  is higher, as the pre-excitation cyclotron radius is inversely proportional to  $B$ . This is specifically helpful to confine very high mass proteins, whose charge state is low, such as those biopolymers, produced by matrix-assisted laser desorption/ionization. There were many developments in the ICR technology at the beginning of the 70s to enable switching the ICR operation mode from variable magnetic strength scans to frequency sweep scans (Comisarow & Marshall, 1974; Hunter & McIver, 1977). Moreover, superconducting magnets represented the next stage of developments over low field electromagnets.

A 4.7-T superconducting magnet was first fitted with a cubic ICR cell, controlled by a Bruker ASPECT 2000 computer in 1980, providing an optimum magnetic field homogeneity, achieved by the help of shim coils (Allemann et al., 1980). A Bruker's ASPECT 2000 computer was capable to run sophisticated electric pulse programs for many important ICR experimental events, such as ion generation, ion quenching, radial ion excitation, and detection. Two modes of operation were introduced since that time allowing the scientist to run ICR experiments in narrowband and broadband ion detection modes.

Frequency sweep was used in broadband mode, whereas single-frequency excitation shot pulse was used in the narrowband mode. Amplification of the induced image currents was subsequently done and an analog to digital converter was used to digitize the acquired time-domain transient, which was also defined as “Fast ion decay” (FID). The ASPECT 2000 computer was capable to perform Fourier-transform from a digitized time-domain transient to a frequency spectrum, which can be subsequently converted to a mass spectrum. In wideband operation mode, a large band excitation frequency range (60 kHz–5 MHz) could be utilized to enable ion detection in a wide mass range (14–1,200)  $m/z$ . When this capability is compared to modern FT-ICR spectrometers, we notice that an extended mass range up to  $m/z$  8,000 can be easily achieved but no low ion masses  $m/z < 100$  can be easily detected with excitation frequencies up to 5 MHz and large magnetic field strengths over 9.4 T, due to reduced ion transmission efficiencies of ions  $< 100 m/z$  in the linear ion beam guide in front of the ICR cell. Given that mass resolution largely increases in an inverse relationship to  $m/z$  ratio, at a low mass detection limit of  $m/z$  14 the theoretical mass-resolving power can reach tens of millions in that 4.7-T FT-ICR-MS instrument, taking full advantage of ICR technology to get a maximum mass resolution for low mass ions.

Another advantage of high field solenoid magnets is the ability to trap an ion inside ICR for a very long period of time. This enables studies of slow gas-phase ion–molecule reactions, with high mass accuracy. The homogeneous field of the 4.7-T solenoid magnet, which was first developed in 1980, was capable to trap tetrachloroethane  $\text{Cl}_2\text{C}=\text{CCl}_2$  ( $m/z$  166) for 13.5 h with 30% ion trapping efficiency at a pressure of  $2 \times 10^{-8}$  Torr. With further enhancements of UHV in the ICR cell, the trapping efficiency can be further enlarged. A titanium sublimation pump, inserted in a liquid nitrogen trap, can be used to achieve lower base pressures. Although ion trapping times over 12 h can be achieved in ICR cells, the detection of ions is confined to a limited transient time which does not exceed few seconds in broadband frequency detection mode and few minutes in narrowband frequency detection mode. Loss of trapped ions during a static trapping event is due to the increase of the magnetron radius, caused mainly by collisions with neutrals (loss of potential). Shortened transient length is due to the decreased cyclotron radius, also caused by collision. Therefore, the lower the pressure the longer becomes the trapping time, and the longer becomes the transient time. The stability of post-excitation ion trajectories is crucial but limited for maintaining long enough recorded time-domain transients for obtaining high frequency and mass-resolving power. This is why the time-domain transient is defined as FID to represent a quick exponential decay of sinusoidal signal within an ICR

ion acquisition. The radial ( $XY$ )-component of the trapping electric field in the ICR cell can negatively affect the stability of trapped ions, which are radially post-excited to the final cyclotron radius for subsequent ion detection. The lower the radial ( $XY$ )-component of the trapping electric field, the higher is the ion stability in its final cyclotron radius during ion detection. Moreover, minimizing space-charge effects also plays a key role to avoid fast time-dependent ion decay of recorded transient, thus enabling higher ion detection sensitivity and higher mass resolution.

In 1983, an ICR experiment in a narrowband frequency excitation mode with the above-mentioned FT-ICR-MS coupled to the 4.7-T Bruker BC-47/89 superconducting magnet, was performed to determine an accurate  $m/z$  of water radical cation (Allemann et al., 1983). A time-domain transient length of 51 s could be digitized and Fourier transformed to yield a mass resolution  $m/\Delta m > 10^8$  for  $m/z$  18 at a pressure of  $8 \times 10^{-11}$  mbar, showing a signal with a very narrow width of 0.04 Hz (FWHM). At that time, it was determined and concluded that ICR experiments lead the best results when the magnetic field strength is fixed and kept homogeneous in the ICR region, whereas a frequency sweep/chirp is used for performing radial excitation of all ions of different  $m/z$  ratios for subsequent ion detection. The 1983 ICR experiment fulfilled these requirements since the residual relative magnetic field variation along the active distance of 4 cm, where the ICR cell is located, was less than  $10^{-5}$ . The high homogeneity of the implemented superconducting magnet enabled achieving such a very high resolution of water radical cations reaching hundreds of millions level. The FT-ICR-MS system was operated by a turbo molecular pump, a titanium sublimation pump with a liquid nitrogen trap, which was used to achieve lower base pressure levels below  $10^{-9}$  mbar.

A wideband frequency mode was also used with the same FT-ICR-MS coupled to the 4.7-T superconducting magnet to measure highly fluorinated positive ions of 2,4,6-tris(nonadecafluorononyl)-1,3,5-triazine with a radical ion  $\text{M}^{\bullet+}$   $m/z$  1,485,  $\text{C}_{30}\text{F}_{57}\text{N}_3$  and  $[\text{M-F}]^+$  at  $m/z$  1,466. This experiment brought in 1983 a clear evidence for the capability of that FT-ICR-MS in achieving very good results in an extended large mass range up to  $m/z$  1,500.

With the same FT-ICR experimental setup, trapping efficiency of 30% of benzene radical ion  $m/z$  78 over 13 h at pressure levels below  $10^{-8}$  mbar was obtained. At the relatively high pressure in ICR, which is usually used to study gas-phase ion–molecule reactions, for 4-min trapping time of benzene ion, a trapping efficiency of 90% at  $1.4 \times 10^{-7}$  mbar was reduced to 80% at  $6.0 \times 10^{-7}$  mbar and was further reduced to 60% efficiency at an extremely high pressure of  $1.4 \times 10^{-6}$  mbar. This shows the

capability of the ICR cell to perform very well, even under extremely high pressure, due to the high magnetic field homogeneity of the 4.7-T superconducting magnet.

### 3 | EXTERNAL ION SOURCE FT-ICR-MS

In the past, researchers utilized FT-ICR-MS for performing fundamental research in the field of gas-phase ion chemistry, studying ion–molecule reactions, obtaining kinetic reaction rate constants, and also studying thermodynamic and electronic properties of reaction intermediates as well as performing fundamental studies to explain electron-impact ionization and its fragmentation mechanisms. Along time, many new applications appeared which require acquiring high mass resolution and accuracy spectra for samples of complex mixtures and matrices. Such applications expand the range of applications from food chemistry, pharmaceutical analysis, forensics, metabolomics, and more recently proteomics and petroleomics. Thus, a strong need emerged for bypassing the limit of ionizing only gaseous analytes and even applying electron impact ionization to solid targets. This could be enabled for the first time in 1985 with the invention of a differentially pumped two-stage FTMS system, which could achieve a three-order of magnitude pressure difference between  $10^{-9}$  mbar in the ICR cell and  $10^{-6}$  mbar in the first vacuum stage, where a solid target probe for electron impact ionization was located.

It is well known that high mass and frequency resolution is linearly proportional to transient length, assuming its full (non-noise) sinusoidal content. To elongate time-domain transients, it is, therefore, crucial to slow down the rate of exponential decay in FID transients. This can be efficiently reached by lowering the base pressure in the ICR region and getting enhanced UHV conditions. Without a differentially pumped multi pressure stages FT-ICR-MS system, it would be impossible to obtain high-resolution mass spectra, especially for solid analytical targets, because they would easily degas quickly, thus preventing from obtaining sufficiently good UHV conditions with a required base pressure in the  $10^{-9}$  mbar range. Thus, a separation between ionization source and the ICR cell used for analysis is the way to provide the required UHV conditions for ICR to deliver ultrahigh-resolution mass spectra. For this purpose, many designs of differentially pumped FTMS were invented.

McIver FTMS design (McIver et al., 1983) utilized quadrupoles to guide the ion beam from the external ionization source through the magnetic fringing fields to the ICR cell. One quadrupole was used for ion transmission and a second quadrupole was used as a mass

filter and also to perform linear collision-induced dissociation (CID) for linearly accelerated ions for MS/MS studies.

A dual ICR cell design was invented by Ghaderi and Littlejohn (1985) to enable externally produced ions to be injected into the ICR analyzer region for ion detection. The dual ICR cell consisted of a source region and an analyzer region and a differential pumping was utilized in the dual ICR cell for achieving UHV in the analyzer ICR. The source region has a higher base pressure relative to the analyzer ICR region and can be used for ion generation by the use of electron impact or laser ionization. A small orifice in an electrode, which separates the two ICR regions from each other allows for ion transfer from the source to the ICR analyzer region for ultrahigh resolution ion detection.

Wanczek et al. (1985) experimentally proved for the first time in 1985 that no specific linear ion beam guides are needed if the pressure difference between the source and analyzer vacuum chambers do not exceed three orders of magnitude. With this design, solid analytical targets could be pumped to  $10^{-6}$  mbar and could then be bombarded with an ionizing electron beam to enable ions to be transferred and subsequently detected in ICR under a  $10^{-9}$ -mbar pressure regime. With only one turbo molecular pump of 50 L/s in the source and one turbo molecular pump of 300 L/s in the analysis region, and an orifice between these two vacuum chambers, inside a 4.7-T magnet, great mass spectra could be achieved. An acetone signal  $S/N = 300$  with  $FWHM = 0.025$  milli  $m/z$  unit could be recorded, yielding a resolution of 1,700,000 at  $m/z$  43. This differentially pumped design could prove its success also in broadband frequency excitation ICR experiments. Solid target EI ionization of many perfluorinated samples of key interest could be recorded. With an ion transmission efficiency above 25% (without any quadrupole and/or other linear ion beam guides), a full  $m/z$  range (18–1,166) could be detected and a high-resolution MS of tris-(perfluoroheptyl)-s-triazine was recorded from a 6.6-ms transient. A resolution of 25,000 could be obtained for a large  $m/z$  1,166 with a 2 s transient. The duty cycle of this design could be characterized by the ionization period in the external ion source and by the time of flight of the transferred ions from the external ion source to the ICR cell.

The trapping time of ions inside the ICR cell in this differentially pumped multi-stage vacuum system was not reduced when a classical single vacuum stage ICR system was utilized for measurements. It should also be mentioned that a high ion transmission efficiency could be achieved taking into consideration the relatively large inhomogeneous fringing magnetic field outside the 4.7-T magnet, where the external ionization source is located.

There is no mass-dependent variation in the linear ion transmission efficiency from the external ion source to the ICR cell along a broad  $m/z$  range (18–1,166) for the inorganic solid samples, mentioned above. Utilizing a smaller orifice between both vacuum chambers and larger turbo molecular pumps can further increase pressure differences between the two vacuum stages. As the external ion source does not have the need to stay under UHV conditions, memory effects are greatly reduced in the acquired FTMS mass spectra.

In 1987, Kofel et al. (1989) further enhanced the external ion source FT-ICR-MS system, developed in 1985 (discussed above), by examining the possibility to trap ions outside of the ICR cell by utilizing the residual magnetic field outside of the magnet border, by taking advantage of the magnetic mirror effect, which can trap ions in the inhomogeneous region outside the ICR cell between it and the external ion source. By applying an electric acceleration pulsed voltage, the ions can be transferred from the trapping and accumulation ion source, positioned directly outside of the room temperature bore of the magnet to the ICR cell for ion detection in high resolution. The yield of detectable ions with this external trapping ion source could be greatly enhanced. The enhanced design consists of an external electron impact ion source located 10 cm outside the border of a 4.7-T superconducting magnet and a 6-cm long ICR cell in the homogeneous magnetic field region inside of that magnet. The EI external ion source was 52 cm far away from the ICR cell. A Faraday cup was used to measure the ions that reached that cup from the ICR cell. A front trapping ICR plate was pulsed to allow ions to enter the ICR cell for a specific period of time and then switched back to the ICR-trapping voltage before radial ion excitation and detection in the ICR cell. The duration of this pulse and the voltages of the external ion source and the transfer voltage were optimized to reach maximum ion transmission efficiency in benzene  $C_6H_6^{\bullet+}$  radical ion experiments. Thirty percent yield could be obtained. Furthermore, Wanczek et al. performed a theoretical study to calculate the maximum  $S/N$  that can be reached in ICR ion detection comparing between four ion FTMS designs: (1) In cell ion generation, (2) dual ICR-cell, (3) external ion source with no quadrupoles, (4) external source with no quadrupoles but with ion trapped and accumulated by the help of the residual magnetic field outside of the magnet. They concluded that an  $S/N$  increase from 140 to 10,000 could be reached by the use of the dual ICR cell when compared with the single ICR cell. The external source with no utilization of the residual magnetic field can give a maximum  $S/N$  of 2,100, which is less than that of the dual ICR cell. However, the best enhancement  $S/N = 350,000$  could be

achieved, when residual magnetic field-assisted ion trapping and accumulation technique was utilized. These results could be obtained after considering the best orifice diameter value of 4 mm, which separates the two cell regions in the dual ICR cell.

#### 4 | TIME OF FLIGHT ICR MASS SPECTROMETRY

In the above-mentioned external ion source ICR design, Kofel et al. (1986b) discovered a time-dependent ion  $m/z$  transfer through the linear flight of ions from the external ion source to the ICR cell. During this linear flight, a free electric field region is passed through by the flying ions. If the initial kinetic energy of the ions is kept constant, time differences of flight as a function of  $m/z$  ratios occur, which enable ions to be separated in arrival time before reaching the ICR cell. This dependency can be implemented to favor effective ion transfer of a specific mass range, which is important to prevent oversaturation of the ICR cell with undesired ions of high abundance. Also in gas chromatography (GC)-MS, carrier gas ions are prevented from entering the ICR cell. The authors of that work implemented a pulsed front trapping ICR cell electrode and investigated in 1986 the effect of changing the duration of the pulse, during which the front ICR-trapping electrode is opened. It was found that the pulse duration should not exceed the ions TOF from the external ion source to the ICR cell, otherwise, ions are lost by their continuous flight beyond the back trapping plate of the ICR cell. Both electron beam pulse duration and the ICR-trapping plate open mode duration can be controlled by a mini-computer and the trapped mass range inside the ICR cell can thus be precisely controlled. The duration of the ionizing electron impact pulse determines the high mass limit, whereas the ICR-trapping plate open-event determines the low  $m/z$  cut-off.

A full theoretical study for the mechanism of trapping ions by the magnetic mirror effect with the solenoid magnetic symmetry around the central magnetic field line ( $z$ -axis) was performed and discussed. Wanczek et al. found in that work, that when ions are linearly accelerated to be transferred from the external ion source toward the ICR cell, the magnetic mirror effect can amplify the energetic motion perpendicular to the magnetic field by a factor over 100. Thus, if the radial kinetic energy of the thermal ions is assumed to be 0.03 eV, then linearly accelerated ions will have a radial enlarged kinetic energy of around 3 eV, perpendicular to the  $z$ -axis of the magnetic field lines. This explains why a portion of the available ions finally reaches the ICR cell, especially, with wide statistical ion thermal velocity distribution. The linear ion transmission efficiency from the external ion source to the ICR cell depends on the

accelerating voltage. Beyond thermal motions, ion radial placement (through motions) may be generated by imperfect electrode arrangement and by space charge of ion packets.

## 5 | Z-AXIS ION EJECTION AND COUPLING OF RADIAL AND AXIAL ION MOTION IN ICR

It was found that during radial ion excitation and in a non-perfect quadrupolar trapping electric potential and non-perfect linear excitation electric potential configuration, the axial and the radial motion of trapped ions inside ICR cells can be coupled. If the excitation frequency is higher than the reduced cyclotron frequency of the trapped ion, the axial motion of the trapped ion inside ICR is excited, which leads to enlarged axial vibrational amplitudes of the trapped ions during excitation until ions can be ejected out of the ICR cell by moving along the central magnetic field line (in the  $z$ -axis) in what is defined as  $z$ -axis ion ejection.

High radial ion excitation levels above one-third of the ICR cell radius are desirable because ion detection sensitivity increase with larger post-excitation cyclotron radii. However, the axial vibrational motion of trapped ions is largely excited with higher radial ion excitation amplitudes in non-perfect electric potential configuration. Thus, a trade-off between high detection sensitivity and low  $z$ -ion ejection phenomenon should be found.

On the contrary, if the excitation RF frequency is lower than the reduced cyclotron frequency of the trapped ion inside the ICR cell, axial ion motion is damped during radial ion excitation. In 1986, Kofel et al. (1986a) suggested that this method can be utilized to damp the axial motion of externally generated and linearly accelerated ions when reaching the ICR cell. A complete theory of ion motion inside a closed cylindrical ICR cell geometry was written in that work. Excellent agreement between predicted signal intensities (according to the mentioned ion motion theory) and the experimental ICR signal intensities was found as a function of excitation frequency and excitation amplitude of a single-frequency excitation pulse.

On the contrary, the  $z$ -axis ion ejection principle can be utilized to selectively eject undesired low mass ions, which exist as a bulk in GC such as the helium ion carrier gas. This is important to increase the dynamic range in ICR ion detection and also to reduce the large adverse space-charge effects that these carrier gas helium ions can cause during ICR ion detection. In a negative ionization mode with electron impact inside ICR cells, undesirable electrons are also co-trapped together with negative ions.

Allemann et al. (1987) performed an extensive theoretical study to calculate the amount of absorbed energy of

trapped ions when they are axially excited by an RF pulse as a function of the irradiated RF frequency on the trapping plates of an ICR cell. They found that the maximum absorbed energy for axial ion excitation along the magnetic field lines is obtained when the irradiated RF frequency is equal to  $2\omega_T$ , where  $\omega_T$  is the trapping frequency of the ion to be ejected along the  $Z$ -axis, where magnetic field lines are centrally located. The phase of that triggered axial RF pulse on one trapping electrode is  $180^\circ$  shifted relative to the other ICR-trapping electrode. This phase shift generates an axial electric force, for selective axial ion ejection of undesired ions. They ran also experiments with trapped helium-positive ions and found out that the largest signal loss of  $\text{He}^+$  could be indeed obtained when the irradiated RF frequency equals to  $2\omega_T$  of the  $\text{He}^+$  ions.

The authors of that study showed important applications of applying the  $z$ -ion ejection by the use of  $2\omega_T$  of trapped ions in ICR to (1) eliminate carrier gas GC helium-positive ions from the ICR cell for generating high dynamic range positive ion mass spectra and in another ICR experiment, (2) to eject successive electrons that may have been trapped together with produced negative ions due to electron impact ionization from the ICR cell. This subsequently reduces space-charge effects and thus increases mass-resolving power for detected trapped anions in negative ion ICR mass spectra.

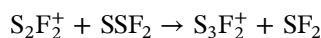
The enhancement in the mass-resolving power was due to the low space-charge effect inside the ICR cell after axial ejection of the remaining electrons from the ICR cell. The authors of that study indicated that there is only one limitation of the implemented axial RF pulse by explaining that axial  $z$ -ion ejection cannot be applied for ICR experiments, where other ions co-exist, whose cyclotron frequencies lie in the same frequency range around the  $2\omega_T$ . However, they proved that such a condition allows for the detection of positive ions with very high  $m/z$  ratios up to 1,400 at a magnetic field strength of 4.7 T in a GC-ICR experiment. Very high  $m/z$  ions ( $m/z > 1,400$ ) do not emerge in GC-FT-ICR-MS when the axial helium ion ejection experiment is applied for effective removal of the carrier gas GC helium-positive ions.

## 6 | ION-MOLECULE REACTIONS IN FT-ICR-MS

The ability of ICR cells to trap reactive ions for a long time was used to study reactions between trapped ions and reactive gaseous compounds. ICR cells can be considered as laboratory test tubes, where diverse gas-phase ion-molecule reactions can be investigated. ICR cells can operate in a high dynamic pressure range from  $10^{-9}$  up to  $10^{-5}$  mbar. With this broad pressure range, both fast and

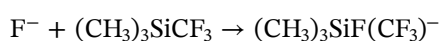
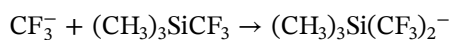
slow ion–molecule reactions can be studied. Fast ion–molecule reactions can be made slow by reducing the base pressure inside the ICR cell. For example, if a reaction takes 1 s to produce product ions at  $1 \times 10^{-7}$  mbar, then the same reaction will require about 10 s to yield the same signal intensity of reaction products at  $1 \times 10^{-8}$  mbar. Reducing the base pressure in the ICR cell has the advantage of significantly increasing the mass-resolving power of the detected reactant and product ions as well as intermediate ions, even though the duration of the reaction increase due to low collision frequency between rotating trapped reactant ions and reactive molecules. For these reactions to progress completely along the reaction coordinate (time), high ion trapping efficiency should be provided and this is exactly what an ICR cell can provide in a highly homogeneous magnetic field. Performing gas-phase ion–molecule reactions in ICR helped also for discovering and investigating new reactive intermediates (Achatz et al., 1999; Jankiewicz et al., 2013; van der Rest et al., 2001; Schröder et al., 1997; Vinueza et al., 2012).

Wanczek et al. (1972) focussed on the non-metal inorganic chemistry of ions and their reactions in ICR. Ion chemistry of thiothionylfluoride was studied and the reaction between  $S_2F_2^+$  and  $S=SF_2$  was observed to yield  $S_3F_2^+$  product ion.



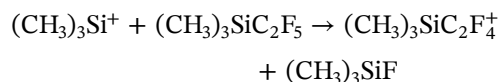
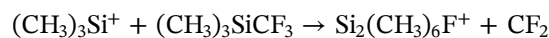
The rate constant of that ion–molecule reaction was determined to  $k = 2 \times 10^{-9} \text{ cm}^3 \text{ molecule}^{-1} \text{ s}^{-1}$ . Many secondary ions were observed:  $S_2F_3^+$ ,  $S_3F^+$ , and  $S_3F_2^+$ . Moreover,  $S_3F_2^+$  can undergo consecutive reactions to yield highly enriched sulfur product ion  $S_4F_2^+$ . Later, these main sulfur isomers: Thiothionylfluorides  $S=SF_2$  and difluorodisulfane FSSF were extensively studied by low-temperature infrared spectrometry (Wanczek et al., 1975) to gain more insight on the mechanism of their rearrangement and decomposition.

Luebkekmann and Wanczek (2008) studied the ion chemistry of key trifluoromethylation agent  $(CH_3)_3SiCF_3$  as well as pentafluoroethylation agent  $(CH_3)_3SiC_2F_5$  and performed density functional theoretical (DFT) calculations, which supported their experimental ICR findings. Penta-coordinated silicon anions could be produced from  $(CH_3)_3SiCF_3$  in addition-type ion–molecule reactions but no such anions could be observed starting from  $(CH_3)_3SiC_2F_5$



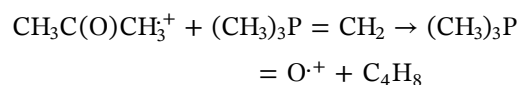
In the positive ion mode, the authors of that study investigated the reactivity of  $(CH_3)_3Si^+$  ion with both

$(CH_3)_3SiCF_3$  and  $(CH_3)_3SiC_2F_5$ . They found that the reactivity of this cation with these two compounds is different:



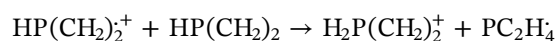
Though a fluorohexamethyldisilane product ion  $Si_2(CH_3)_6F^+$  is observed as a result of the ion–molecule reaction of trimethylsilylium cation with  $(CH_3)_3SiCF_3$ , a fluoride anion transfer ion–molecule reaction is revealed in case of the reaction of the trimethylsilylium cation with  $(CH_3)_3SiC_2F_5$ .

Hartmann et al. (1976) studied the ion chemistry of trimethylmethylenephosphorane and its important Wittig reaction when its reactive anions are let to react with acetone in ICR. Only the acetone molecular cation was reactive when it was let to react with the yield  $(CH_3)_3P=CH_2$ , but the  $(CH_3)_3P=CH_2^+$  was not reactive toward acetone neutrals.

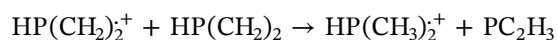


It was concluded that the ylide loses its reactivity with ketones, when it is being ionized to yield a radical cation.

Gas-phase ion chemistry of phosphorous compounds in ICR was also the main focus of Wanczek's and Hartmann's groups. They studied the ion chemistry of phosphirane (Profous et al., 1975) and determined the structure of its positive ion to be indeed cyclic. Pressure dependence of signal intensities of the reactive ions for both phosphirane and methylphosphine was studied. Significant differences in ICR pressure dependency of the signal intensities between phosphirane and methylphosphine could be experimentally revealed and explained. Double-resonance ICR experiments confirmed the lack of charge transfer reactions in the case of phosphirane gas-phase ion chemistry. The main ion–molecule reactions of phosphirane can be proposed and their rate constants were determined, as follows:



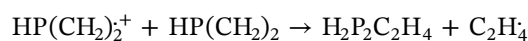
$$k = 0.54 \times 10^{-10} \text{ cm}^3 \text{ molecule}^{-1} \text{ s}^{-1},$$



$$k = 0.80 \times 10^{-10} \text{ cm}^3 \text{ molecule}^{-1} \text{ s}^{-1}$$



$$k = 0.50 \times 10^{-10} \text{ cm}^3 \text{ molecule}^{-1} \text{ s}^{-1}$$

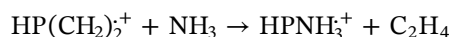
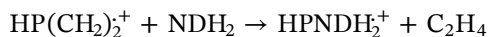
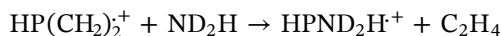
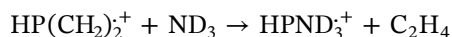


$$k = 0.77 \times 10^{-10} \text{ cm}^3 \text{ molecule}^{-1} \text{ s}^{-1}.$$

The ring-opening reaction ( $k = 0.80 \times 10^{-10} \text{ cm}^3 \text{ molecule}^{-1} \text{ s}^{-1}$ ) proceeds significantly faster than the

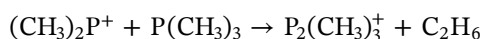
protonation reaction of phosphirane ( $k = 0.54 \times 10^{-10} \text{ cm}^3 \text{ molecule}^{-1} \text{ s}^{-1}$ ).

In the same work, Profous et al. studied also the ion chemistry of phosphirane in the presence of  $\text{ND}_3$ ,  $\text{NHD}_2$ ,  $\text{NH}_2\text{D}$ , and ammonia.

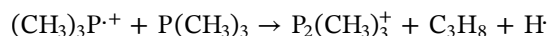


According to the above-mentioned ion-molecule reactions of the phosphirane radical ion with  $\text{ND}_3$ ,  $\text{NHD}_2$ ,  $\text{NH}_2\text{D}$ , and ammonia, the authors concluded that no H/D scrambling takes place in the gas-phase when these above-mentioned product ions are formed.

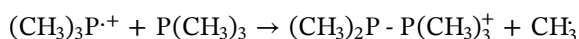
In another study, Wanczek and Profous (1975) performed extensive study of the ion chemistry of trimethylphosphine. Sixty gas-phase ion-molecule reactions could be revealed in that study with the help of ICR. New ions with a direct covalent P-P bond could be formed by reacting the dimethylphosphine ion (which presents the base peak in the mass spectrum of trimethylphosphine) with the trimethylphosphine neutrals.



In these reactions, which yield a P-P covalent bond, an electrophilic attack of the ionic phosphorous reactant on the nucleophilic phosphorus atom in trimethylphosphine takes place. Not only addition reaction but also phosphonium ion transfer reaction can take place as illustrated by the ability of  $(\text{CH}_3)_3\text{P}^+$  to react with trimethylphosphine neutrals to form a dimethyldiphosphenium product ion with a direct P-P bond.

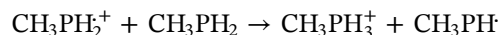


In that study, it was found that there is another reaction channel for the reactants  $(\text{CH}_3)_3\text{P}^+$  and  $\text{P}(\text{CH}_3)_3$  to form pentamethyldiphosphenium ion. No hexamethyldiphosphenium product ion could be stabilized in the gas-phase under the used ICR pressure conditions so that the following reaction is considered a displacement reaction, due to the release of a methyl radical and this was the main ion-molecule reaction of the molecular ion.

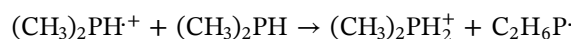


Wanczek also generated ICR mass spectra of methylphosphine, dimethylphosphine, and dimethyldeutero-phosphine and studied their gas-phase ion chemistry (Wanczek, 1975). Signal intensities of produced EI ions were

plotted against ICR pressure in the range  $10^{-6}$  to  $10^{-4}$  Torr and 50 ion-molecule reactions could be observed for each compound. These reactions are classified to yield phosphonium ions with two or three phosphorous atoms, as well as charge exchange reactions and CIDs. The rate constants of protonation of methylphosphine and dimethylphosphine were determined as shown in the following reactions. The protonation reaction is faster when the phosphorus atom in the phosphine has more P-H bonds.

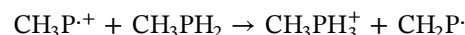


$$k = 8.2 \times 10^{-10} \text{ cm}^3 \text{ molecule}^{-1} \text{ sec}^{-1}$$

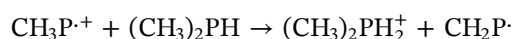


$$k = 1.4 \times 10^{-10} \text{ cm}^3 \text{ molecule}^{-1} \text{ sec}^{-1}$$

Protonation of phosphines can also occur by the use of the less reactive  $\text{CH}_3\text{P}^+$  radical cation. Again the protonation rate constant decreases further with less P-H bonds.

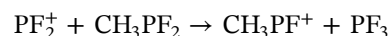


$$k = 3.7 \times 10^{-10} \text{ cm}^3 \text{ molecule}^{-1} \text{ sec}^{-1}$$

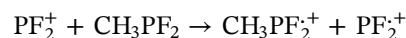


$$k = 0.1 \times 10^{-10} \text{ cm}^3 \text{ molecule}^{-1} \text{ sec}^{-1}$$

Not only different methylated phosphine derivatives were subject to intensive ICR studies but also fluorinated and trifluoromethylated phosphines. An extensive review of versatile ion-molecule reactions of phosphorous as well as fluorinated phosphorous compounds was recently published (Wanczek & Kanawati, 2019). Wanczek and Rösenthaller (1976) studied the ICR mass spectra and ion chemistry of dimethylfluorophosphine and methyl-difluorophosphine, and determined their appearance potentials. The ionization potential for methyl-difluorophosphine was determined to be 9.8 eV and for dimethylfluorophosphine was determined to be 8.9 eV. The base peak in the ICR-MS of methyl-difluorophosphine is  $\text{PF}_2^+$ , which can further react with the  $\text{CH}_3\text{PF}_2$  neutrals within the scope of a fluoride anion transfer reaction:

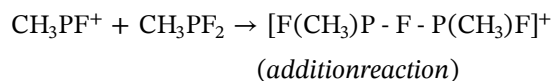
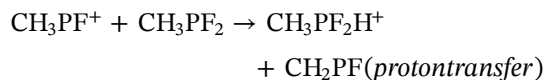


A charge transfer reaction was also observed to produce  $\text{CH}_3\text{PF}_2^+$ .

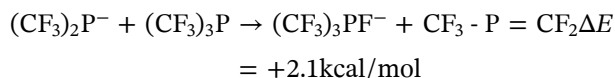


$\text{CH}_3\text{PF}^+$  is a reactive ion and it can react with methyl-difluorophosphine in three reaction channels:

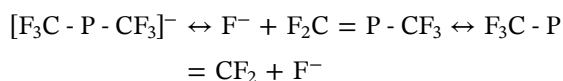




Kanawati and Wanczek (2007b) showed that it is possible to produce many phosphoranide anions  $(\text{CF}_3)_3\text{PF}^-$ ,  $(\text{CF}_3)_2\text{PF}_2^-$ , and  $\text{CF}_3\text{PF}_3^-$  in the study of the ion chemistry of tris(trifluoromethyl)phosphine in ICR. Negative ionization of  $(\text{CF}_3)_3\text{P}$  by thermal electron attachment produces a phosphide anion  $(\text{CF}_3)_2\text{P}^-$ , which is considered as a decomposition product anion of  $(\text{CF}_3)_3\text{P}^{\bullet-}$  because the radical molecular ion  $(\text{CF}_3)_3\text{P}^{\bullet-}$  is unstable and it undergoes a rapid methyl radical elimination to produce the phosphide anion. The phosphide anion  $(\text{CF}_3)_2\text{P}^-$  is a strong nucleophile and the phosphorus atom bears two electron lone pairs. When the phosphide anion is accelerated inside the ICR cell, by applying an on-resonance radial dipolar ion excitation RF-pulse, several phosphoranide product anions can be produced according to the following scheme:

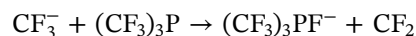


Kanawati and Wanczek (2014) revealed the reaction mechanism in detail by the DFT and found that this ion-molecule reaction is slightly endothermic. Thus, acceleration of the trapped phosphide anion is definitely necessary to produce a high yield of the main phosphoranide product anion  $(\text{CF}_3)_3\text{PF}^-$ . The authors also revealed that the phosphide anion is a fluoride anion donor, due to stabilization of the remaining neutral (due to electron delocalization) as shown in this equation:



The main produced phosphoranide anion  $(\text{CF}_3)_3\text{PF}^-$  can undergo CID to form  $(\text{CF}_3)_2\text{PF}_2^-$  and  $\text{CF}_3\text{PF}_3^-$  by successive difluorocarbene  $\text{CF}_2$  eliminations. The energy barriers for these successive  $\text{CF}_2$  eliminations were also calculated by DFT. The authors could confirm that the phosphoranide anion  $(\text{CF}_3)_3\text{PF}^-$  cannot be used as a  $\text{CF}_3$  transfer agent, as activation of that phosphoranide anion would favor the above-mentioned successive elimination of  $\text{CF}_2$ . These results about the reactivity of this phosphoranide were later confirmed in solution (Shyshkov, 2006). Furthermore, no indication of any produced anion with a P-P covalent bond could be observed in the ion chemistry of  $(\text{CF}_3)_3\text{P}$  studied by ICR even at relatively elevated pressure levels in the range  $10^{-8}$ – $10^{-6}$  mbar. This could be understood because the  $\text{CF}_3$  groups around

phosphorous would reduce the electron density needed for a P-P covalent bond to be established. Furthermore, ion-molecule reaction between  $\text{CF}_3^-$  and  $(\text{CF}_3)_3\text{P}$  was also studied, but no route to  $(\text{CF}_3)_4\text{P}^-$  phosphoranide ion was found. The authors could reveal the mechanism for that ion-molecule reaction by DFT and could identify the transition state, which drives this reaction to add only one fluoride anion and eliminate  $\text{CF}_2$



Thus, a fluoride anion transfer instead of  $\text{CF}_3^-$  addition occurs, indicating that the largest phosphoranide that can be prepared from tris(trifluoromethyl)phosphide is actually the  $(\text{CF}_3)_3\text{PF}^-$  anion.

## 7 | DUAL ION POLARITY ICR CELLS AND LONG-RANGE ION-ION INTERACTIONS

Starting from 1992, researchers came out with several ideas to enable simultaneous trapping and detection of positive and negative ions in ICR cells. Gorshkov et al. enabled in 1992 simultaneous trapping and detection of positive and negative ions inside a cubic ICR cell by applying an alternating RF field on the ICR-trapping end caps (Gorshkov et al., 1992). The axial ion motion is governed by a Mathieu equation, providing an ion stability region around  $q_z = 4q\gamma V_{\text{ac}}/(m\Omega^2) = 0.5$ , where  $m/q$  is the mass to charge ratio,  $\Omega$  is the driving frequency of the alternating axial electric field,  $V_{\text{ac}}$  is the voltage of that RF field and  $\gamma = 2.7737/d^2$ ,  $d$  is the edge length of the cubic ICR. The authors found that a triangular RF waveform is more effective than a sinusoidal one and could trap both positive and negative ions but the sensitivity of this trapping is limited to those ions with specific  $m/z$  ratios, whose Mathieu  $q_z$  stability parameter is equivalent to and located in the range  $0.4 \leq q_z \leq 0.7$ .

Wang and Wanczek invented in 1992 the first ICR cell, which could trap and detect both positive and negative ions without the need for any axial alternating RF field (Wang & Wanczek, 1993). Only DC-trapping potentials were applied. A grid in front of each trapping plate in a cylindrical ICR cell allowed the generation of three potential extrema. Ions of both polarities could be stored at different sites in the ICR, excited and reacted, and detected. With this invention they could overcome the restriction of ion trapping to the above-mentioned Mathieu  $q_z$  stability parameter range. Sulfur hexafluoride ICR experiments were done and  $\text{SF}_5^+$  and  $\text{SF}_6^-$  could be efficiently trapped and simultaneously detected.

Before 1992, an ICR study by Rempel and Gross in 1991 (Rempel & Gross, 1992) was done to assess the

applicability of an RF-trapping field to enable ion trapping and detection of key metastable product ions, which could only be stabilized by high collision frequency of buffer gas helium atoms under extremely high pressure ( $10^{-3}$  mbar) inside the ICR cell. For this purpose and to enable efficient ion stability inside ICR under such extreme pressure conditions, dynamic ion trapping was implemented in an event, which takes place after the helium pulsed valve is closed and an additional long time is waited for pumping down the ICR cell back to  $10^{-7}$  mbar before acquisition.

Vartanian and Laude (1994) developed a nested multi-section cylindrical cell to trap and detect both positive and negative ions. Multiple electric well/hill potential configurations can be programmed for this purpose. Both  $\text{Cl}^-$  and  $\text{CH}_2\text{Cl}^+$  fragment ions, produced as a result of electron impact ionization of chloroform could be detected. In another experiment of IR laser ablation on KCl attached onto a gold target,  $\text{Au}^+$ ,  $\text{K}^+$ , as well as  $\text{Cl}^-$ , could simultaneously be trapped and detected in their ICR cell.

Malek and Wanczek (1996) performed further extensive ICR studies on simultaneous positive and negative ion trapping and detection. They characterized a cylindrical cell with double (grid and plate)-trapping electrodes and calculated the electric potential inside the cell by a Fourier–Bessel series expansion method. With electron impact ionization of a mixture of sulfur hexafluoride and xenon and with the application of a double-hill electric potential configuration, both  $\text{Xe}^{2+}$  and  $\text{SF}_6^-$  could be trapped and detected simultaneously in that ICR cell. Charge selective ion ejection experiments could also be performed. The authors also performed recombination experiments of  $\text{Ar}^+$  ions with electrons in that cell.

Lobodin et al. (2013) developed a cylindrical ICR cell with seven ring electrodes. This cell improved the generation of potential extrema and the reaction of trapped particles. With this cell, neutralization and charge reduction reactions were studied. The authors provided with this design the first tandem in time charge reversal ICR experiments by the use of high-energetic electrons/UV laser photons. Neutralization–reionization experiments were possible with energetic UV photons. Negative fullerene anions were trapped in both terminal ICR regions in a double-hill electric potential configuration. As soon as a charge inversion from negative to positive ion formation occurs, the produced positive fullerene ions fall in the central electric potential well, suitable for trapping positive ions. Dynamic trapping of both ion polarities was also implemented for these experiments.

An open cylindrical ICR cell, with several terminal-trapping electrodes of different diameters, was invented

and thoroughly examined (Kanawati & Wanczek, 2007a). Experiments with this cell confirmed its potential to trap positive and negative ions in a double-well electric potential configuration for relatively long trapping times of over 15 s at high pressure  $2 \times 10^{-6}$  mbar. Extensive SIMION simulations were also performed on that cell to study the 3D characteristics of the double-well electric potential configuration, used for trapping and detection of both positive and negative ions. These simulations also confirmed for the first time that this cell is capable of establishing different final post-excitation cyclotron radii when positive ions are compared to negative ions after applying a standard dipolar radial ion excitation scheme. The reason for this difference in the post-excitation cyclotron radii was discerned by calculation of the maximum kinetic energy, that can be absorbed, for ions trapped in central and terminal stability regions, during the dipolar radial excitation event. Moreover, a significant difference in the extent of the radial acceleration component of ions stored in different axial stability regions along the double-hill electric potential configuration was observed. A non-linear radial acceleration component was found for those ions, trapped on terminal stability regions (near the trapping tubes). The degree of radial positive–negative ion separation is dependent on the amplitude of the dipolar radial electric excitation field. The flexibility of this new nested trapping ICR cell was also shown in the fact that it is possible to shift the terminal electric potential maxima, which normally trap negative ions, in the above-mentioned double-hill electric potential configuration to be located deep inside the detection region of the ICR cell so that both central positive and terminal negative ions can be efficiently detected after post-excitation of both ion polarities.

Ion–ion interaction experiments between centrally trapped  $\text{SF}_3^+$  and terminally trapped  $\text{SF}_6^-$  ions in the above-mentioned ICR cell were performed by applying a single-shot pulse, which applies a change of the double-hill electric potential configuration (Kanawati & Wanczek, 2008b), during which the terminally trapped  $\text{SF}_6^-$  ions are axially inwardly pushed (accelerated) toward the center of the ICR cell. High ion densities were found to be a prerequisite for effective ion–ion interactions. No electron transfer could be indicated at a pressure of  $10^{-7}$  mbar but anion–anion collisions could be revealed by SIMION ion trajectory simulations. When the ICR cell pressure is increased to  $10^{-6}$  mbar in the same above-mentioned single-shot experiment, a noticeable decrease in the signal intensity of the centrally trapped  $\text{SF}_3^+$  ions could be observed, during inward terminal  $\text{SF}_6^-$  ion acceleration toward the centrally trapped  $\text{SF}_3^+$  ions. Thus, the role of the pressure in the ICR cell region was confirmed, so that high pressure

(>10<sup>-5</sup> mbar) relative to what generally prevails and required for ICR operation is necessary to mediate effective ion–ion reactions through third body collisions. Distortion of radial ion trajectories of centrally trapped positive ions could be indicated when both central positive and terminally trapped negative ions were excited simultaneously through radial dipolar ion excitation. By controlling the electric potentials of the trapping tubes, it is possible to further push terminally trapped ions inside the detection region toward the center of the cell for further enhanced ion detection sensitivity.

In another experiment, Kanawati and Wanczek (2008a) found out that, long-range ion–ion interactions could be achieved by the implementation of more sophisticated different RF waveform pulses with different frequencies, which periodically change the axial electric potential of the multi-segmented ICR cell of different diameters. This enabled longer continuous electrostatic mutual interaction between ions of different polarities, to move beyond the previously mentioned single-shot change of the axial electric potential configuration. In an ion–ion ICR experiment between centrally trapped SF<sub>5</sub><sup>+</sup> and terminally trapped SF<sub>6</sub><sup>-</sup> ions in a double-hill electric potential configuration and when the centrally trapped positive ions are outward excited axially by on-resonance RF sinusoidal modulation pulse, it was observed that the axially excited SF<sub>5</sub><sup>+</sup> ions are not lost from the ICR cell when SF<sub>6</sub><sup>-</sup> ions are co-trapped. Centrally trapped SF<sub>5</sub><sup>+</sup> can be lost with this on-resonance axial sinusoidal RF waveform if no SF<sub>6</sub><sup>-</sup> anions are co-trapped (terminally) in the cell. This brought strong experimental evidence that axially outward excited central SF<sub>5</sub><sup>+</sup> ions meet the terminally trapped SF<sub>6</sub><sup>-</sup> ions and a long-range ion–ion attracting interaction between these different ion polarities occurs near the inner edges of the side electrodes (inside the detection region of the ICR cell). These long-range attractive ion–ion interactions are not sufficient (at such a low pressure of 10<sup>-7</sup> mbar) to initiate an electron transfer. However, such an interaction can further trap the axially excited central SF<sub>5</sub><sup>+</sup> ions and prevent their ejection out of the ICR cell, so that SF<sub>5</sub><sup>+</sup> ions can still be detected in a substantial abundance after the end of the above-mentioned on-resonance axial sinusoidal excitation pulse. The same authors of that study also assessed the applicability of applying a square RF waveform at the main frequency, which is on-resonance with the centrally trapped SF<sub>5</sub><sup>+</sup> ions, to further study possible ion–ion interactions. However, they found that the square waveform at that main frequency was not helpful, because a marginal sideband of such a square waveform exists at a frequency, which lies 1.3 kHz off-resonance to the cyclotron frequency of the terminally trapped SF<sub>6</sub><sup>-</sup> ions. This caused slight radial expansion in

the cyclotron radius of the SF<sub>6</sub><sup>-</sup> ions during the application of that square RF waveform pulse, so that no ion–ion collisions could be made feasible. Such differences in the radial ion expansion patterns between centrally trapped positive ions and terminally trapped negative ions, which were axially pushed against each other by applying a periodic square waveform pulse were responsible for the absence of an electron-transfer reaction.

Investigations of gas-phase ion–ion interactions inspired many researchers to perform further experiments in relatively higher-pressure conditions (higher than what prevails in ICR experiments) and electron transfer ion–ion reactions could be indeed achieved in ion traps with trapping pressures four to five orders of magnitude higher than in the ICR experiments. A very interesting application for these reactions is electron transfer dissociation (ETD) for sequencing of protein ions in mass spectrometry (Riley & Coon, 2018; Syka et al., 2004) although ETD has drawbacks with insufficient dissociation of doubly charged protein precursor ions (Swaney et al., 2007).

## 8 | CONCLUSION

In this review, a brief account is given focusing especially on the studies performed in Wanczek's group and the ICR research laboratory at the University of Bremen. Many instrumental developments were accomplished in many aspects of the ICR technology. Several new ICR cells were invented and thoroughly characterized. Analytical solutions to the ion motion under the influence of homogeneous magnetic and inhomogeneous trapping electric field (Hartmann et al., 1983) were obtained and extensive SIMION ion trajectory simulations to study ion motion and plot important physical characteristics, such as spatial electric potential distribution, which guide the 3D ion motion, were done. External ion sources were developed and an emphasis on the use of superconducting magnets is made, showing many great advantages with ion trapping efficiency exceeding 13.5 h at 4.7 T. The transition from magnetic sweep to frequency sweep marked one of the most key developments in the ICR technology, before the invention of FT-ICR. Developments of dual polarities ICR cells for simultaneous trapping and detection of both positive and negative ions enabled studying of ion–ion long-range interactions. Gas-phase ion–molecule reactions were intensively studied focusing on many inorganic compounds with sulfur, silicon, and phosphorous atoms. The rate constant of many

ion–molecule reactions could also be experimentally determined in ICR.

## REFERENCES

- Achatz U., Beyer M., Joos S., Fox B. S., Niedner-Schattenburg G., Bondybey V.E., 1999, *J. Phys. Chem. A*, 103: 8200–8206.
- Allemann M., Kellerhals H. P., Wanczek K. P. 1980. *Chem. Phys. Lett.* 75: 328–331.
- Allemann M., Kellerhals H. P., Wanczek K. P. 1983. *Int. J. Mass Spectrom. Ion Proc.* 46: 139–142.
- Allemann M., Kofel P., Kellerhals H. P., Wanczek K. P. 1987. *Int. J. Mass Spectrom. Ion Proc.* 74: 47–54.
- Comisarow M. B., Marshall A. G. 1974. *Chem. Phys. Lett.* 25: 282.
- Forcisi S., Moritz F., Kanawati B., Tziotis D., Lehmann R., Schmitt-Kopplin P. 2013, Liquid chromatography–mass spectrometry in metabolomics research: Mass analyzers in ultra high pressure liquid chromatography coupling. *J. Chrom. A*, 1292: 51–65.
- Ghaderi S., Littlejohn D. P. 1985. Proc. 33rd Annu. Conf. Mass Spectrom. Allied Top., San Diego, C.A., p. 727.
- Gorshkov M. V., Guan S., Marshall A. G. 1992. Dynamic ion trapping for Fourier transform ion cyclotron resonance mass spectrometry: simultaneous positive and negative ion detection, *Rapid Comm. Mass Spectrom.* 6: 166–172.
- Hartmann H., Chung K. M., Schuch D., Wanczek K. P. 1980, On the Coriolis coupling of ion cyclotron motion to ion internal degrees of freedom. *Int. J. Mass Spectrom. Ion Proc.* 34: 303–310.
- Hartmann H., Chung K. M., Baykut G., Wanczek K. P. 1983. Dependence of ion cyclotron frequency on electric field inhomogeneity. *J. Chem. Phys.* 78: 424–431.
- Hartmann H., Lebert K.-H., Wanczek K. P. 1973, Ion cyclotron resonance spectroscopy, *Top. Curr. Chem.* 43: 57–115.
- Hartmann H., Wanczek K. P., (Eds). 1978. Ion cyclotron resonance spectrometry, *Lecture Notes Chem.* Vol. 7.
- Hartmann H., Wanczek K. P. (Eds.). 1982. Ion cyclotron resonance spectrometry II, *Lecture Notes Chem.* Vol. 31.
- Hartmann O. R., Wanczek K-P., Hartmann H. 1976. Ion-molecule reactions of trimethylenephosphorane and its mixture with acetone, investigated by ion cyclotron resonance spectrometry. In: *Advances in Mass Spectrometry, Vol. 7A, Proceedings of the 7th international mass spectrometry conference held at Florence*, 274–279.
- Hendrickson, C. L., Emmett, M. R. 1999. Electrospray ionization Fourier transform ion cyclotron resonance mass spectrometry, *Annual Rev. Phys. Chem.* 50: 517–536.
- Hunter R. L., McIver R. T. Jr. 1977. *Chem. Phys. Lett.* 49: 577.
- Jankiewicz B. J., Vinuesa N. R., Kirkpatrick L. M., Gallardo V. A., Li G., Nash J. J., Kenttämaa H. I. 2013, Does the 2,6-didehydropyridinium cation exist? *J. Phys. Org. Chem.* 26: 707–714.
- Kanawati B., Wanczek K. P. 2007a. Characterization of a new open cylindrical ion cyclotron resonance cell with unusual geometry, *Rev. Sci. Instrum.* 78: 074102.
- Kanawati B., Wanczek K. P. 2007b. Gas phase FT ICR investigation of the production of phosphoranides and ion chemistry of tris (trifluoromethyl)phosphine, *Int. J. Mass Spectrom.* 264: 164–174.
- Kanawati B., Wanczek K. P. 2008a. RF-driven ion–ion long-range interaction in a new open cylindrical ICR cell, *Int. J. Mass Spectrom.* 274: 30–47.
- Kanawati B., Wanczek K. P. 2008b. Characterization of a new open cylindrical ICR cell for ion–ion collision studies, *Int. J. Mass Spectrom.* 269: 12–23.
- Kanawati B., Wanczek K. P. 2014. Phosphoranide production and decomposition in the gas phase, *Int. J. Mass Spectrom.* 362: 18–23.
- Kanawati B., Wanczek K. P., Schmitt-Kopplin P. 2019. Chapter 6: “Data Processing and Automation in Fourier Transform Mass Spectrometry”, in: “*Fundamentals and Applications of Fourier transform mass spectrometry*”, Elsevier.
- Kofel P., Allemann M., Kellerhals H. P., Wanczek K. P. 1986a. *Int. J. Mass Spectrom. Ion Proc.* 74: 1–12.
- Kofel P., Allemann M., Kellerhals H. P., Wanczek K. P. 1986b. *Int. J. Mass Spectrom. Ion Proc.* 72: 53–61.
- Kofel P., Allemann M., Kellerhals H. P., Wanczek K. P. 1989. *Int. J. Mass Spectrom. Ion Proc.* 87: 237–247.
- Lee S. H., Wanczek K. P., Hartmann H. 1980. *Adv. Mass Spectrom.* 8B: 1645–1649.
- Lobodin V. V., Savory J. J., Kaiser N. K., Dunk P. W., Marshall A.G. 2013. Charge reversal Fourier transform ion cyclotron resonance mass spectrometry, *J. Am. Soc. Mass Spectrom.* 24: 213–221.
- Luebkekmann F., Wanczek K. P. 2008. Gas phase ion chemistry of (CH<sub>3</sub>)<sub>3</sub>SiCF<sub>3</sub> and (CH<sub>3</sub>)<sub>3</sub>SiC<sub>2</sub>F<sub>5</sub>, FT-ICR experiments and theory, *Int. J. Mass Spectrom.* 278: 95–100.
- Malek R., Wanczek K. P. 1996. FT-ICR mass spectrometry with simultaneous trapping of positive and negative ions, *Int. J. Mass Spectrom. Ion Proc.* 157/158: 199–214.
- Marshall A. G., Chen T. 2015. 40 years of ion cyclotron resonance mass spectrometry. *Int. J. Mass Spectrom.* 377: 410–420.
- Marshall A. G., Hendrickson C. L. 2002. Fourier transform ion cyclotron resonance detection: principles and experimental configurations. *International Journal of Mass Spectrometry* 215: 59–75.
- Marshall A. G., Hendrickson C. L. 2008. High-resolution mass spectrometers, *Ann. Rev. Anal. Chem.* 1: 579–599.
- Marshall A. G., Hendrickson C. L., Jackson G. S. 1998. Fourier transform ion cyclotron resonance mass spectrometry: A primer. *Mass Spectrom. Rev.* 17: 1–35.
- McIver R. T., Hunter R. L., Story M. S., Syka J., Labunsky M., 1983. Proc. 31st Annu. Conf. Mass Spectrom. Allied Top., Boston, USA.
- Nikolaev E. N., Gorshkov M. V., Mordehai A. V., Talrose V. L. 1985, Multi-electrode detection FT ICR cell, patent application, *Soviet Union SU 1307492 A1*.
- Nikolaev E. N., Kostyukevich Y. I., G. N. Vladimirov 2016. Fourier transform ion cyclotron resonance (FT ICR) mass spectrometry: Theory and simulations. *Mass Spectrom. Rev.* 35: 219–258.
- Nolting D., Malek R., Makarov A. 2019. Ion traps in modern mass spectrometry. *Mass Spec Rev.* 38: 150–168.
- Profous Z. C., Wanczek K. P., Hartmann H. 1975. *Z. Naturforsch.* 30a: 1470–1475.
- Rempel D. L., Gross M. L. 1992, *J. Am. Soc. Mass Soc.* 3: 590.
- van der Rest G., Chamot-Rooke J., Mourgues P., McMahon T. B., Audier H. E. 2001, Ter-body intermediates in the gas phase: Reaction of ionized enols with tert-butanol. *J Am Soc Mass Spectrom.* 12: 938–947

- Riley N. M., Coon J. J., 2018. The role of electron transfer dissociation in modern proteomics. *Anal. Chem.* 90: 40–64.
- Schröder D., Schwarz H., Clemmer D. E., Chen Y., Armentrout P. B., Baranov V. I., Böhme D. K., Activation of hydrogen and methane by thermalized FeO<sup>+</sup> in the gas phase as studied by multiple mass spectrometric techniques. 1997. *Int. J. Mass Spectrom.* 278: 95–100.
- Schweikhard L., Blundschling M., Jertz R., Kluge, H. J. 1989. A new detection scheme for Fourier transform-ion cyclotron resonance spectrometry in Penning traps, *Rev. Sci. Instrum.* 60: 2631–2634.
- Schweikhard L., Lindinger M., Kluge H. J. 1990. *Int. J. Mass Spectrom. Ion Proc.* 98: 25–33.
- Shyshkov O., 2006. URN: urn:nbn:de:gbv:46-diss000105080 (PhD thesis), University of Bremen.
- Swaney D. L., McAlister G. C., Wirtala M., Schwartz J. C., Syka J., Coon J. J. 2007. Supplemental activation Method for high-efficiency electron-transfer dissociation of doubly protonated peptide precursors. *Anal. Chem.* 79: 477–485.
- Syka J., Coon J., Schroeder M., Shabanowitz J., Hunt D. 2004. Peptide and protein sequence analysis by electron transfer dissociation mass spectrometry, *Proc. Natl. Acad. Sci.* 101: 9528–9533.
- Vartanian V. H., Laude D. A. 1994. Simultaneous trapping of positive and negative ions using a nested open-ended trapped ion cell in Fourier transform ion cyclotron resonance mass spectrometry, *Org. Mass Spectrom.* 29: 692–694.
- Vinueza N. R., Archibold E. F., Jankiewicz B. J., Gallardo V. A., Habicht S. C., Aqueel M. S., Nash J. J., Kenttämää H. I. 2012. Reactivity of the 4,5-didehydroisoquinolinium cation. *Chem. Eur. J.* 18: 8692–8698.
- Wanczek K. P. 1975. *Z. Naturforsch.* 30a: 329–339.
- Wanczek K. P. 1982, Ion cyclotron resonance spectrometry: a review on instrumentation and theory, *Dynamic Mass Spectrom.* 6: 14–32.
- Wanczek K. P. 1989, ICR spectrometry—A review of new developments in theory, instrumentation, and applications. I. 1983–1986, *Int. J. Mass Spectrom. Ion Proc.* 95: 1–38.
- Wanczek K. P., Bliefert C., Budenz R. 1975. *Z. Naturforsch.* 30a: 1156–1163.
- Wanczek K. P., Kanawati B. 2019. Chapter 18: “ Gas Phase Ion-Molecule Reactions of Inorganic Compounds in FT-ICR-MS”, In: “*Fundamentals and Applications of Fourier transform mass spectrometry*”, Elsevier.
- Wanczek K. P., Kofel P., Allemann M., Kellerhals H. P. 1985. *Int. J. Mass Spectrom. Ion Proc.* 65: 97–103.
- Wanczek K. P., Lebert K. H., Hartmann H. 1972. *Z. Naturforsch.* 271: 155–158.
- Wanczek K. P., Profous Z. C. 1975. *Int. J. Mass Spectrom. Ion Proc.* 17: 23–38.
- Wanczek K.-P. Röschenhaler G.-V. 1976. Mass spectra and ion-molecule reactions of dimethylfluorophosphine and methyl difluorophosphine, investigated by ion cyclotron resonance spectrometry, In: *Dynamic mass spectrometry*, 4, Chapter 11: 163–174.
- Wang Y., Wanczek K. P. 1993. A new ion cyclotron resonance cell for simultaneous trapping of positive and negative ions, *Rev. Sci. Instrum.* 64: 883–889.
- Zhang L. K., Rempel D., Pramanik B. N. 2005. Accurate mass measurements by Fourier transform mass spectrometry. *Mass Spectrom. Rev.* 24: 286–309.

## AUTHOR BIOGRAPHIES



**Karl Peter Wanczek** studied chemistry at the university of Saarbrücken. He received his PhD in 1970 with the work on inorganic sulfur fluorine compounds in the group of Prof. Dr. F. Seel, Institut of Inorganic Chemistry. As a postdoc he joined the group of Prof. Dr. H. Hartmann, Institutes of Physical and Theoretical Chemistry at the University of Frankfurt. During this time he started his work on ICR spectrometry. In 1976 he was appointed Professor of Chemistry at the University of Bremen. He retired in 2005. His continuing research interests are: ICR spectrometry, instrumentation development and fundamentals of ion-molecule reactions mainly of simple phosphorus compounds.



**Basem Kanawati** holds a Bachelor degree of science from the University of Damascus, Syria and a Diploma in Chemistry from the University of Bremen, Germany. He did his PhD in the field of physical inorganic chemistry and FT-ICR mass spectrometry under the supervision of Prof. Dr. Karl Peter Wanczek in the University of Bremen. As a Postdoc, he joined Max Planck Institute of Chemistry in Mainz, Germany to study environmental aerosols and moved to Helmholtz Zentrum München. His research interests are: Ultra-high resolution mass spectrometry, physical organic chemistry, computational chemistry, instrumental developments and digital signal processing.

**How to cite this article:** Wanczek KP, Kanawati B. FT-ICR mass spectrometry: Superconducting magnet, external ion source, ion-molecule reactions, and ion-ion traps. *Mass Spec Rev.* 2021;1–14. <https://doi.org/10.1002/mas.21682>